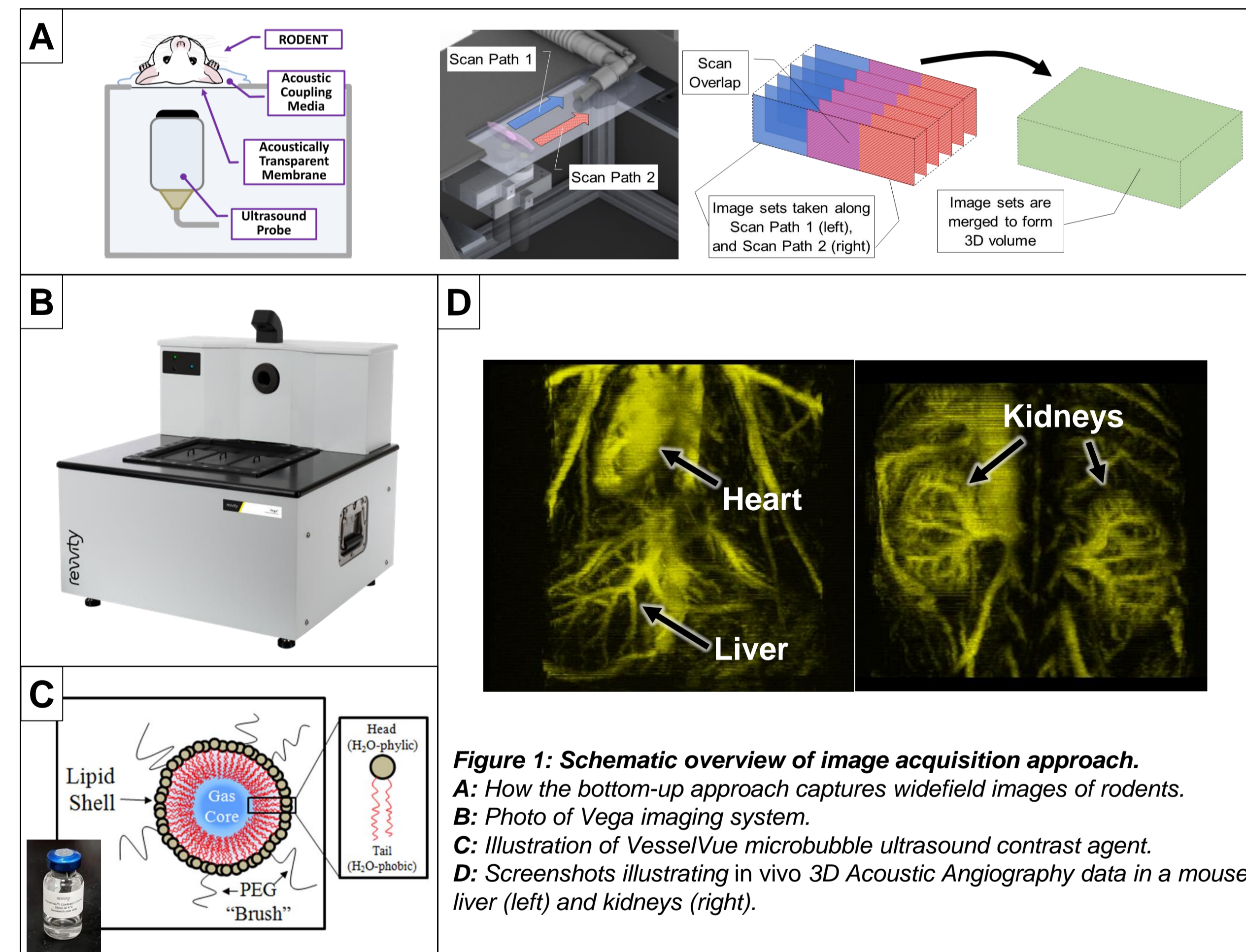


1 Background

- Glioblastoma (GBM) is the most common primary brain tumor with <5% of patients surviving >5 years post diagnosis.
- Murine models play a vital role in researching new treatment options for GBM.
- Small animal MRI is the most common and sensitive method for noninvasively tracking GBM tumors in rodent models, however it is costly and time consuming, which makes large cohort studies challenging.
- Ultrasound imaging offers a cost-effective and high-throughput alternative, but historically struggles as a brain imaging modality due to poor skull penetration and low contrast

GOAL: To evaluate a new 3D contrast-enhanced ultrasound imaging approach for rapidly measuring tumor volumes *in vivo* in rodent models for GBM.

2 Imaging Methods



3 Study Design

6-week old female athymic nude mice were implanted with U87 GMB cells in the brain.

Implantation. Cells (3 μ L total injection volume) were implanted on the left side of the brain approximately 0.6 mm anterior from bregma, 2 mm lateral from center, and 3 mm from the surface of the brain using a stereotaxic stage, motorized micromanipulator, and microinjection syringe pump.

- Round 1- 6 mice were implanted with 1×10^5 cells.
- Round 2- 8 mice were implanted with 1.5×10^5 cells.

Imaging. Mice were imaged with both US and MRI twice per week for 4 weeks after implantation, starting 1 week after implantation, with the following imaging parameters:

- US: Acoustic Angiography images were acquired using the Density preset in SonoEQ with an additional 20 sec delay between repetitions. A 1:1 mixture of VesselVue and saline was injected via continuous infusion pump (30 μ L bolus followed by 15 μ L/min after).
- MRI: 9.4T T2 images were acquired using a 100 μ m and 250 μ m in-plane and out-of-plane resolution, respectively, and 6 repetitions.

4 Representative Images

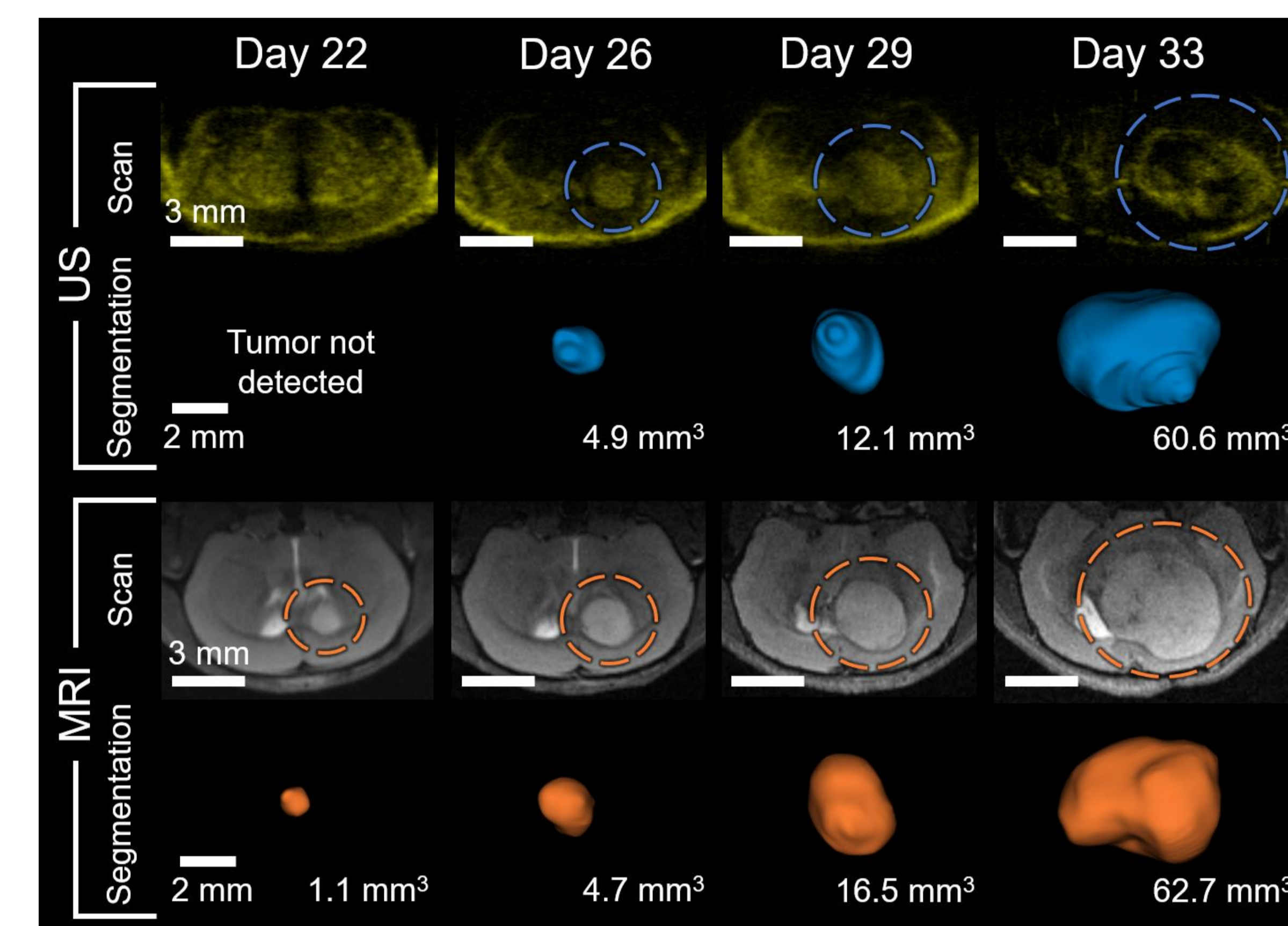


Figure 2: Representative tumor growth images of US (top row) and MRI (third row). The 3D rendering of the segmentations are shown in rows 2 and 4 for US and MRI, respectively. Tumor location is indicated by the dotted circles.

5 Longitudinal Growth Curves

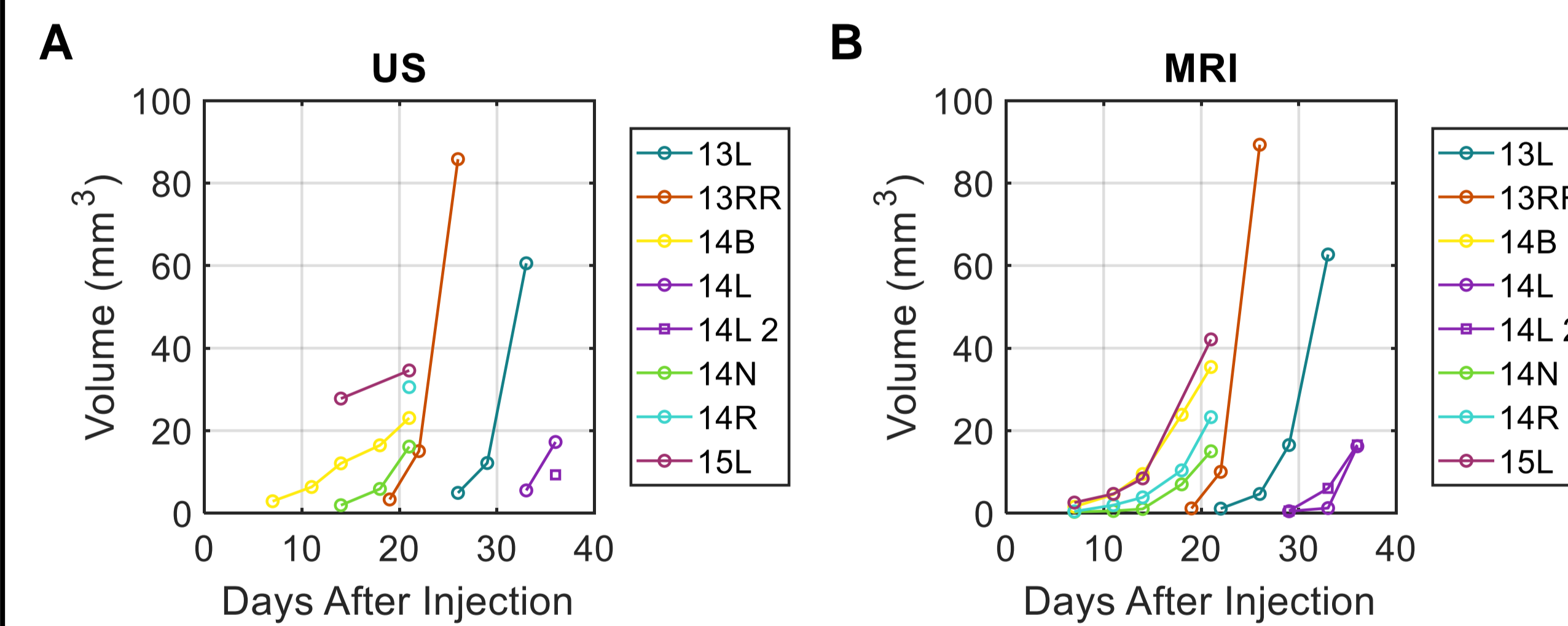


Figure 3: Tumor volume over time for US (A) and MRI (B). All tumors from round 2 were detected by MRI 7 days after implantation, except in one case where the mouse did not grow a tumor. Only 3 mice from round 1 grew tumors and were detected by MRI 19, 22, and 29 days after implantation. Furthermore, the growth curves measured by US and MRI are similar for tumors that US detected in multiple timepoints.

6 Correlation Analysis

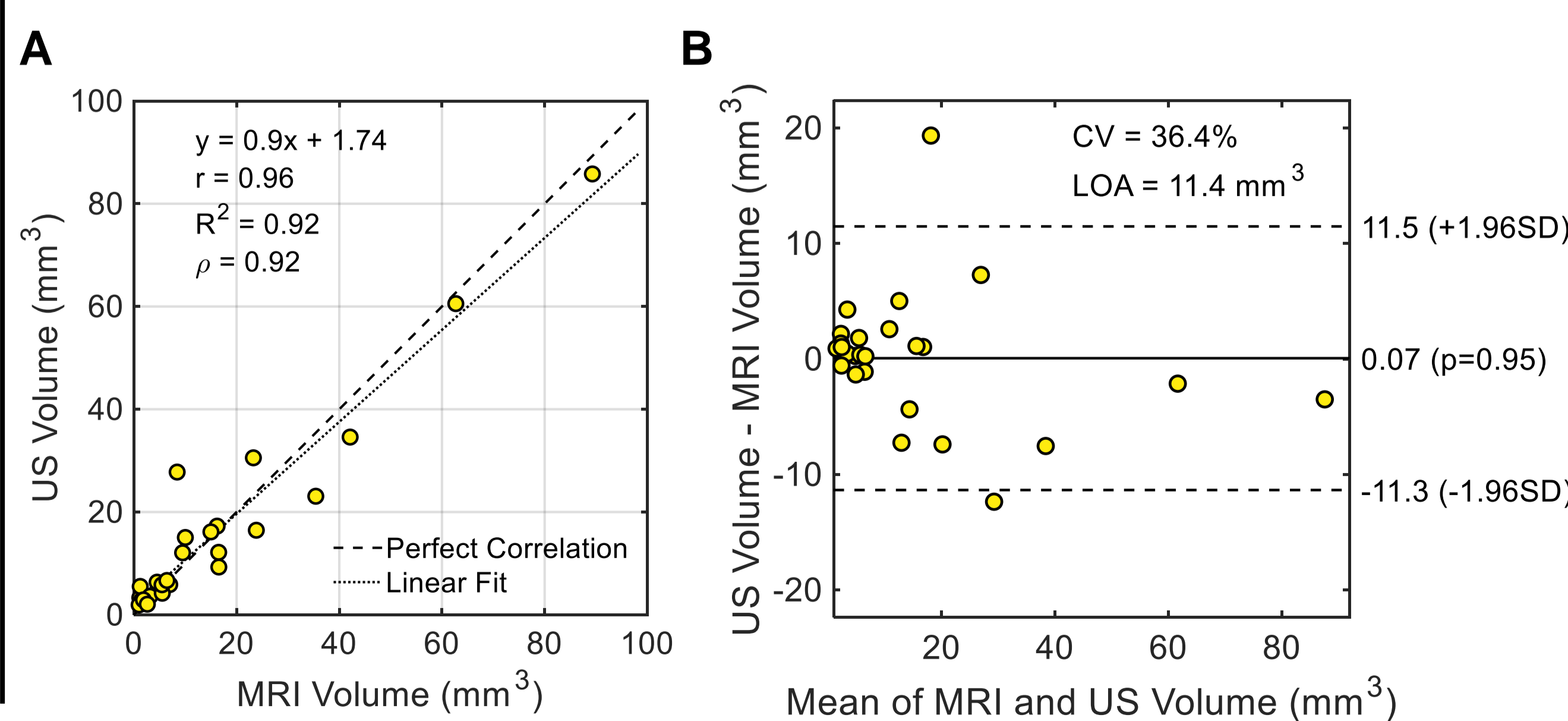


Figure 4: Correlation (A) and Bland-Altman (B) plots of US vs MRI volume measurements. r -Pearson correlation coefficient, R^2 -coefficient of determination, p -Spearman correlation coefficient, CV-coefficient of variation, LOA-limits of agreement.

7 Limits of Detectability

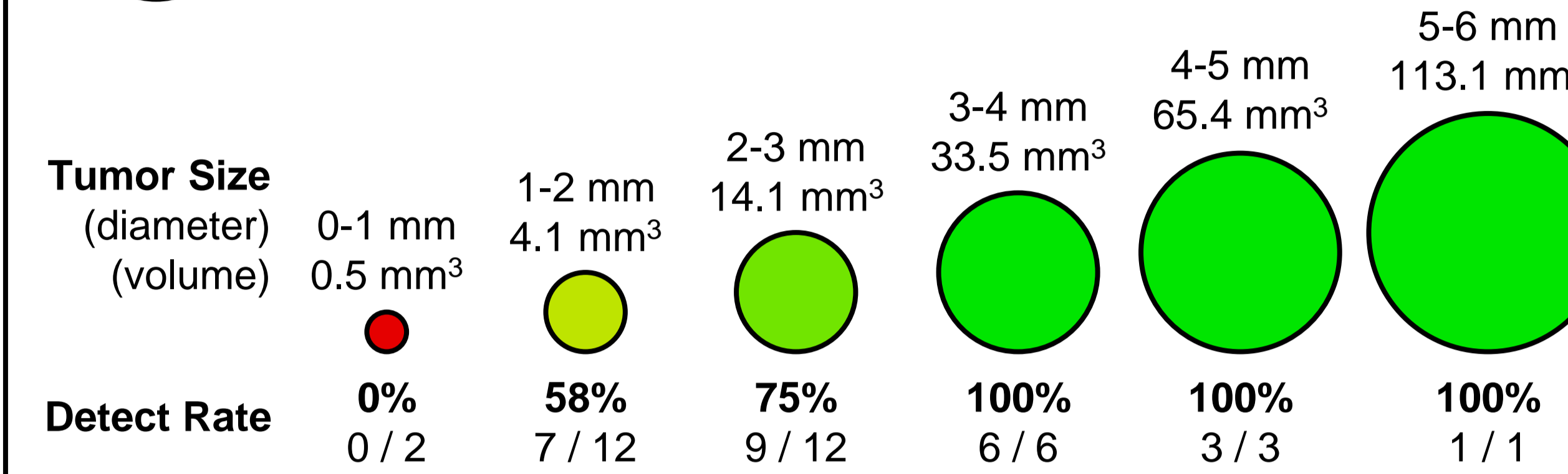


Figure 5: Detection rate versus tumor size. For illustrative purposes, edges of histogram bins are defined as incremental spheroid diameters with tumor volume cut-points computed as $\frac{4}{3}\pi r^3$. US detected 72.2% (26 out of 36) of the tumors that were seen in MRI. The mean volume, as measured by MRI, of tumors that were missed by US was 2.3 mm^3 , while the mean volume of tumors that were detected by US was (8.0 mm^3). Smaller tumors were more easily detected in US images in areas of the brain with lower baseline AA signal (suggesting higher difference in vascular density between diseased and healthy brain tissue).

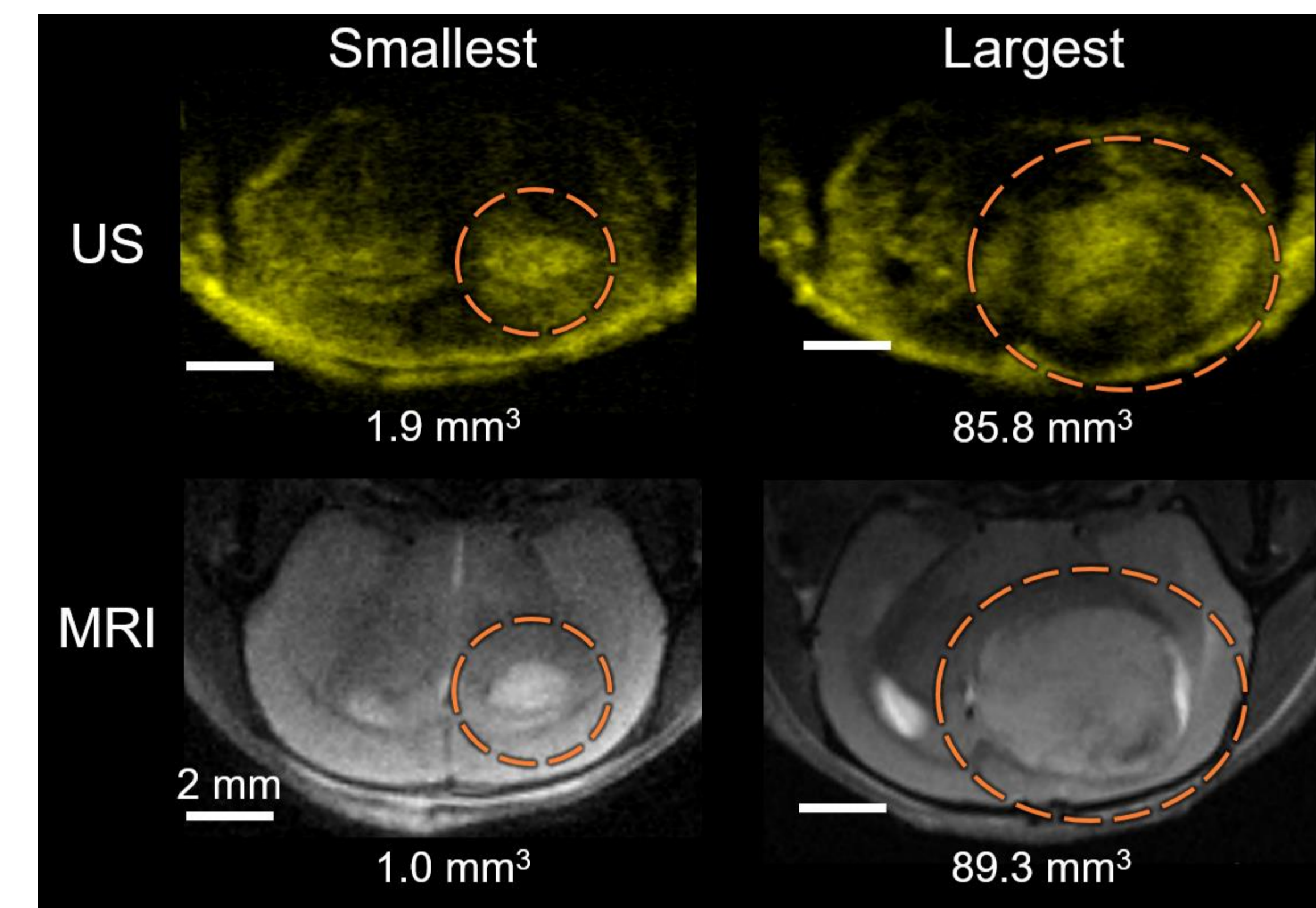


Figure 6: US (top) and MRI (bottom) images of the smallest (left) and largest (right) tumors that were detected by US.

8 Tumor Growth Location

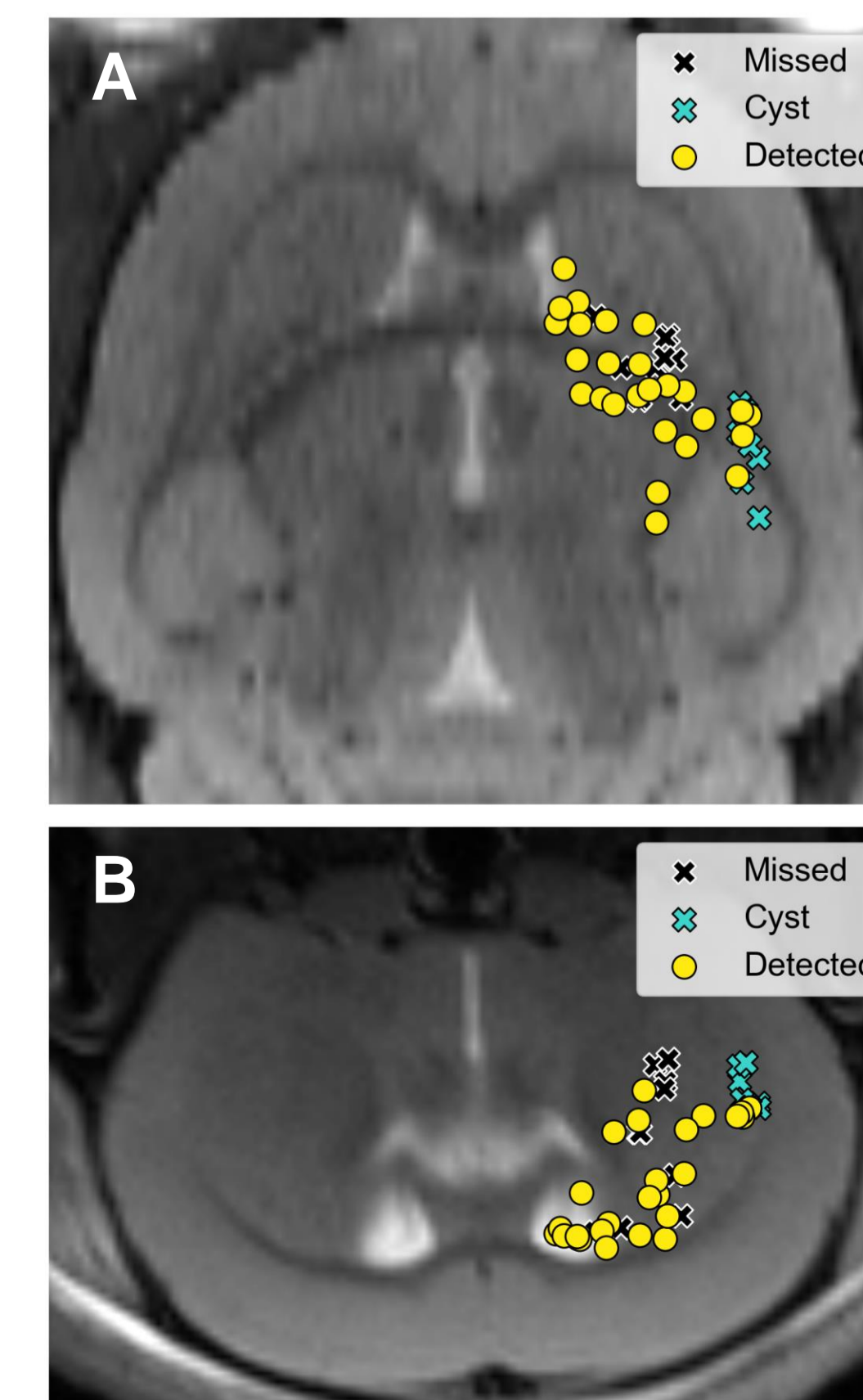


Figure 7: Tumor center locations overlaid on MRI images of a healthy brain in the coronal (A) and axial (B) orientations. Center locations of tumors that were detected by US are depicted by yellow circles, while the locations of cysts and tumors not detected by US are shown as teal and black X's, respectively. The axial location is 0.6 mm caudal from Bregma and the coronal plane is 3 mm from the top of the brain. No pattern was found to explain why some of the tumors were not detected by US.

9 Outlier Examples

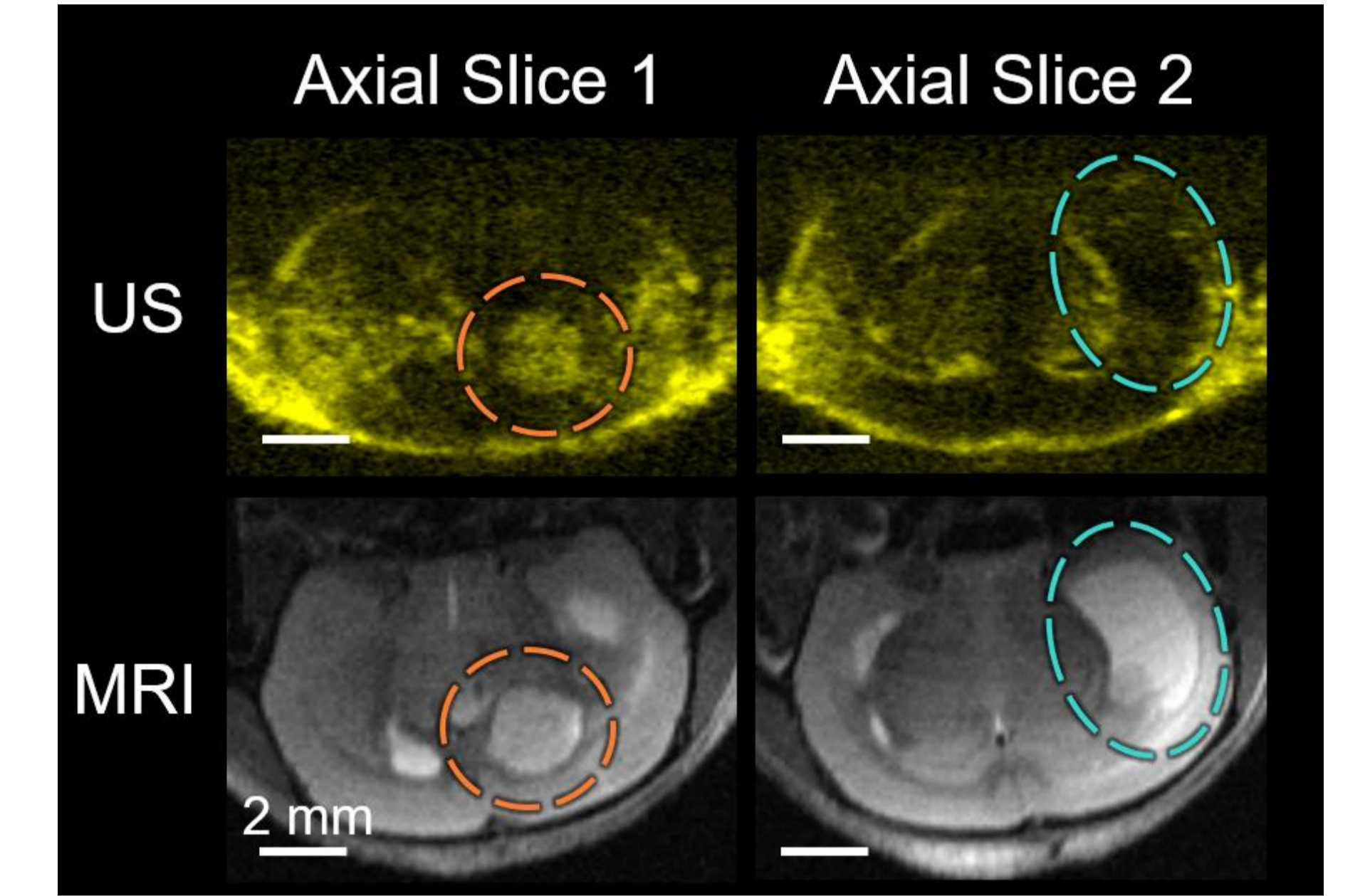


Figure 8: US (top) and MRI (bottom) images of a brain where one axial location contained a tumor (left) and the other a cyst (right). The tumor and cyst appear similar on MRI, while the tumor and cyst are hyperechoic and hypoechoic, respectively, in the US image. Cysts were excluded from the analysis.

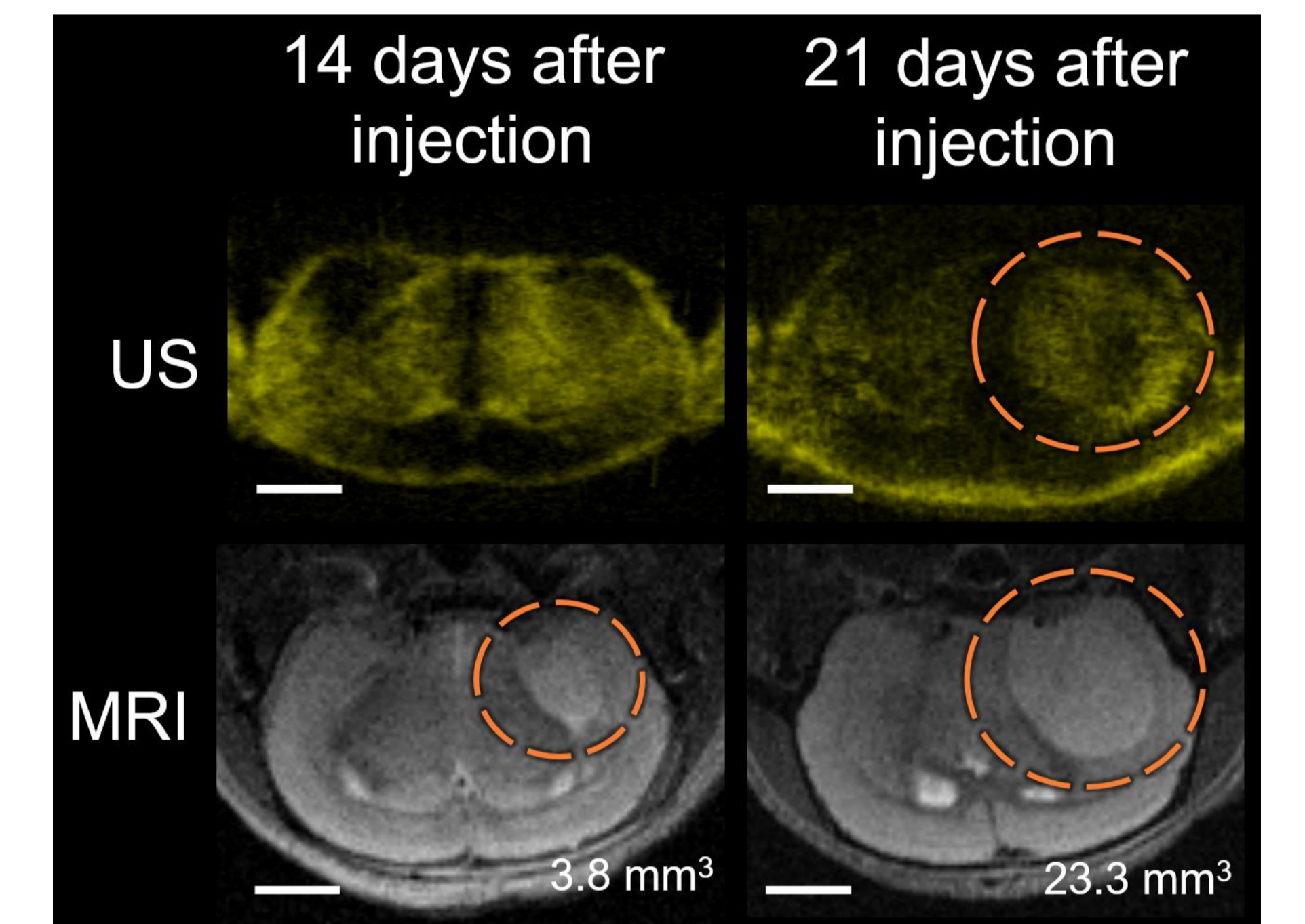


Figure 9: US (top) and MRI (bottom) images of a tumor that was not detected with US until the last imaging timepoint. US detected several tumors that were smaller than 5 mm^3 but failed to detect some that were twice that size.

10 Conclusions

These studies demonstrate that the ultrasound (US) technique of Acoustic Angiography has the potential to be used for tracking glioblastoma development in mice. While US was not able to detect as many tumors as MRI, the volume measurements obtained on detected tumors had a strong correlation ($R^2 = 0.92$) between US and MRI.

Future work will focus on optimizing US imaging parameters to improve sensitivity and enhance detection. Furthermore, histology will be performed to explore why some tumors were not detected by US.

Funding sources: NIH R44CA239830

Corresponding Author: Tomek Czernuszewicz, Ph.D. tomasz.czernuszewicz@revvity.com